Image Segmentation Using a Multilayer Level-Set Approach *

Jason Chung and Luminita Vese†

UCLA C.A.M. Report 03-53, September 2003, updated June 2005

Abstract

This paper is devoted to piecewise-constant segmentation of images, using a curve evolution approach in a variational formulation. The problem to be solved is also called the minimal partition problem, as formulated by Mumford and Shah [26]. The proposed new models can be viewed as extensions of the techniques previously introduced in [10], [11], [35]. In this present paper, we represent the set of boundaries of the segmentation implicitly, by a multilayer of level-lines of a continuous function. In the standard approach of front propagation, only one level line is used to represent the boundary. The multilayer idea is inspired from previous work on island dynamics for epitaxial growth [5], [13]. Using a multilayer level set approach, the computational cost is smaller. Also, in some applications, a nested structure of the level lines can be useful.

Keywords: functional minimization, free boundary problem, multilayer implicit representation, level sets, image segmentation, partitioning.

Contents

*This work has been supported in part by the National Science Foundation (Grant # NSF-ITR ACI-0113439) and by the National Institute of Mental Health and the National Institute of Neurological Disorders and Stroke (Grant # MH65166).

†J. Chung and L. Vese are with the University of California, Los Angeles, Department of Mathematics. E-mail: senninha@math.ucla.edu, lvese@math.ucla.edu.

1 Introduction

We model here images by functions $f : \Omega \to I\!R$, where Ω is an open and bounded domain in $I\!R^n$. In particular, $n = 1$ corresponds to signals, $n = 2$ corresponds to planar images, while $n = 3$ corresponds to volumetric images, such as MRI data.

An important problem in image analysis is the segmentation or the partition of an image f into regions and their boundaries, such that the regions correspond to objects in the scene. Here, we deal with the case where we look for an optimal piecewise-constant approximation of the function f, our starting point being the minimal partition problem, as formulated by D. Mumford and J. Shah [26]. The general problem is, given a function f in $L^\infty(\Omega)$ (induced by the L^2-topology), find a set of disjoint open regions Ω_i, such that $u = c_i$ in each Ω_i is a minimizer of [26]

$$F(u, \Gamma) = \sum_i \int_{\Omega_i} |f - c_i|^2 dx + \mu \mathcal{H}^{n-1}(\Gamma), \tag{1}$$

where $\Gamma = \cup \partial\Omega_i$, $\Omega = \cup \Omega_i \cup \Gamma$, $\mu > 0$ is a scale parameter, and $\mathcal{H}^{n-1}$ is the Hausdorff $(n-1)$-dimensional measure in $I\!R^n$. The existence of minimizers has been proved by Mumford-Shah for continuous data f [26], and later by Congedo-Tamanini [14] and independently by Morel-Solimini [24], for data $f \in L^\infty(\Omega)$. Elliptic convergent approximations of the minimal partition problem in the weak formulation (and also of the full Mumford and Shah model) have been proposed by Ambrosio-Tortorelli [2], [3], where the minimizer u is approximated by smoother functions, and the unknown set of discontinuities is also approximated by a smooth function v, essentially supported outside Γ. A constructive convergent algorithm for solving (1) has been proposed by Koepfler-Lopez-Morel [18], based on region merging (a piecewise-constant minimizer u is obtained, and not only a smooth approximation).

Also, it has been proved by Mumford-Shah [26] that a minimizer u of (1) has a finite number of regions Ω_i and of constant intensities c_i.

Curve evolution techniques and implicit representations [28], [27] have been proposed to solve particular cases of the minimal partition problem, where the number of regions Ω_i or an upper bound are assumed to be known. Thus, in [10], [11], [35], [36], restrictions of the energy (1) to piecewise-constant functions taking a finite number of regions and intensities, in a variational level set approach, have been considered. The energy has been minimized for restrictions to $\{u(x) = c_1 H(\phi(x)) + c_2 H(-\phi(x))\}$, or $\{u(x) = c_{11} H(\phi_1(x)) H(\phi_2(x)) + c_{10} H(\phi_1(x)) H(-\phi_2(x)) + c_{01} H(-\phi_1(x)) H(\phi_2(x)) + c_{00} H(-\phi_1(x)) H(-\phi_2(x))\}$, and so on, where $\phi, \phi_i : \Omega \to I\!R$ are Lipschitz continuous functions, and H denotes the Heaviside function. The variational level set approach from [37] has been used, together with the level set method [28]. The boundaries were represented by zero level lines of ϕ_i.

The multiphase formulation from [37] has been used in [32], [33] for computing the boundaries $\partial\Omega_i$ in the case of a finite and known number of regions, and where the corresponding intensity averages c_i where given.

The advantage of the multiphase method in [35] is that triple junctions can be represented, as in [37], [32], [33], but the regions Ω_i are disjoint and covering of Ω by definition. In addition, a smaller number of level set functions ϕ_i was needed to represent the partition, for the same number of distinct intensities c_i.

In the above mentioned work, together with other related work, the unknown boundaries $\partial\Omega_i$ are represented by the zero level line of a Lipschitz continuous function ϕ. In general, such function $\phi : \Omega \to I\!R$, as used for active contours [6], [19], [7], [17] partitions the domain Ω in at most two open regions $\{x \in \Omega : \ \phi(x) > 0\}$ and $\{x \in \Omega : \ \phi(x) < 0\}$, with a common boundary given by the zero level line of ϕ, $\{x \in \Omega : \ \phi(x) = 0\}$. For image partition, active contours, and image segmentation, such functions ϕ are thus used to represent boundaries of regions of different characteristics. In order to represent more than two regions, several functions ϕ_i can be combined and used, as we have mentioned in [37], [32], [33], [35]. For instance, in [35], only two functions ϕ_i, $i = 1, 2$ were used to represent up to four disjoint regions making up Ω, and only three functions ϕ_i, $i = 1, 2, 3$ were used to represent up to eight disjoint regions.

Here, we continue the approaches from [10], [11], [35], and we show that we can use even fewer level set functions to represent disjoint regions making up Ω. The applications illustrated in this paper include active contours for object detection, image segmentation and image partition, image denoising. The main idea is to use more than one level of the Lipschitz continuous function ϕ to represent the discontinuity set of u. Thus, the computational cost is decreased, due to less expensive storage. The idea is inspired from a different application of implicit curve evolution and free boundaries, introduced in [5], [13], where island dynamics for epitaxial growth is modeled. A first layer of islands is represented by $\{x : \ \phi(x) = 0\}$, then a second layer of islands, growing on the top of the previous one is represented as $\{x : \ \phi(x) = 1\}$, etc.

In summary, here we combine the techniques from [10], [11], [35] for image partition, with the multilayer technique for modeling epitaxial growth from [5], [13], to obtain new and improved curve evolution models for image segmentation. A recent independent work for image segmentation is presented in [20], where the authors propose an interesting and efficient multi-phase image segmentation model, following [35], but different than the methods proposed in the present work.

The proposed minimization methods are non-convex, and with no uniqueness for global minimizers (these theoretical properties are inherited from the Mumford and Shah model). Moreover, we do not guarantee that our multilayer formulation computes a global minimizer of the energy. It is possible sometime to obtain only a local minimizer by the computational algorithm. Also, the final result may depend on the choice of the initialization. However, in practice, we have obtained very satisfactory results; the numerical algorithm is stable and the computed energy is decreasing function of iterations, to a local or global minimizer.

Related prior work for region based segmentation using the level set method is by Paragios-Deriche [29], [30], [31], and by Tsai, Yezzi and Willsky [34], among other work mentioned in [35].

2 Description of the proposed models

2.1 The case of one function

We consider in this subsection the case when the contours in the image f can be represented by level lines of the same level set function ϕ.

2.1.1 Two levels

Let us consider a Lipschitz continuous function $\phi : \Omega \to I\!R$. Using for instance two levels $l_1 = 0$ and $l_2 = l > 0$, the function ϕ partitions the domain into three disjoint open regions, making up Ω, together with their boundaries:

$$\begin{aligned} R_1 &= \{x \in \Omega : \ \phi(x) < 0\}, \\ R_2 &= \{x \in \Omega : \ 0 < \phi(x) < l\}, \\ R_3 &= \{x \in \Omega : \ \phi(x) > l\}. \end{aligned}$$

We can thus extend the binary piecewise-constant level set segmentation model from [10], [11], to the following model, again as an energy minimization algorithm, in a level set form:

$$\begin{aligned} \inf_{c_1,c_2,c_3,\phi} F(c_1,c_2,c_3,\phi) = &\int_\Omega |f(x) - c_1|^2 H(-\phi(x))dx \\ &+ \int_\Omega |f(x) - c_2|^2 H(\phi(x))H(l - \phi(x))dx \\ &+ \int_\Omega |f(x) - c_3|^2 H(\phi(x) - l)dx \\ &+ \mu\Big[\int_\Omega |\nabla H(\phi)| + \int_\Omega |\nabla H(\phi - l)|\Big], \end{aligned} \tag{2}$$

where H is the one-dimensional Heaviside function, and $\mu > 0$ is a weight parameter. The terms $\int_\Omega |\nabla H(\phi)|$ and $\int_\Omega |\nabla H(\phi - l)|$ correspond to the length of the boundary between R_1, R_2 and R_2, R_3, respectively.

The segmented image in this case will be given by

$$u(x) = c_1 H(-\phi(x)) + c_2 H(\phi(x))H(l - \phi(x)) + c_3 H(\phi(x) - l).$$

To minimize the above energy, we approximate the Heaviside function by a regularized version H_ε, as $\varepsilon \to 0$, such that $H_\varepsilon \to H$ pointwise and $H_\varepsilon \in C^1(I\!R)$. We denote by $\delta_\varepsilon := H'_\varepsilon$. Examples of such approximations, that we use in practice, are [10], [11]:

$$H_\varepsilon(z) = \frac{1}{2}\Big(1 + \frac{2}{\pi} arctan(\frac{z}{\varepsilon})\Big), \quad \delta_\varepsilon(z) = \frac{1}{\pi} \cdot \frac{\varepsilon}{\varepsilon^2 + z^2}.$$

Minimizing now the corresponding approximate energy F_ε alternately with respect to the unknowns, yields the associated Euler-Lagrange equations, parameterizing the descent

direction by an artificial time $t \geq 0$:

$$\phi(0,x) = \phi_0(x), \tag{3}$$

$$c_1(t) = \frac{\int_\Omega f(x)H(-\phi(t,x))dx}{\int_\Omega H(-\phi(t,x))dx}, \tag{4}$$

$$c_2(t) = \frac{\int_\Omega f(x)H(\phi(t,x))H(l-\phi(t,x))dx}{\int_\Omega H(\phi(t,x))H(l-\phi(t,x))dx}, \tag{5}$$

$$c_3(t) = \frac{\int_\Omega f(x)H(\phi(t,x)-l)dx}{\int_\Omega H(\phi(t,x)-l)dx}, \tag{6}$$

$$\frac{\partial \phi}{\partial t} = \tag{7}$$

$$\delta_\varepsilon(\phi)\Big[|f-c_1|^2 - |f-c_2|^2 H(l-\phi) + \mu \mathrm{div}\Big(\frac{\nabla\phi}{|\nabla\phi|}\Big)\Big]$$

$$+\delta_\varepsilon(\phi-l)\Big[H(\phi)|f-c_2|^2 - |f-c_3|^2 + \mu \mathrm{div}\Big(\frac{\nabla\phi}{|\nabla\phi|}\Big)\Big].$$

$$\frac{(\delta_\varepsilon(\phi)+\delta_\varepsilon(\phi-l))\nabla\phi}{|\nabla\phi|}\cdot\vec{n} = 0 \text{ on } \partial\Omega, \ t>0, \tag{8}$$

where $\vec{n}$ is the exterior unit normal to $\partial\Omega$. At steady state, a local or global minimizer of the energy (2) will be obtained.

We will show in the Appendix that the energy $F(c_1(t), c_2(t), c_3(t), \phi(t,\cdot))$ is decreasing in time, under the flow (3)-(8). Also, existence and approximation results and the numerical discretization are also given in the Appendix. Note that the energy (2) is non-convex and it may have more than one global minimizer, these being properties inherited from the Mumford and Shah model. In practice, we do not guarantee that our computational algorithm converges to a global minimizer. Therefore, sometime only a local minimizer may be obtained, but close to a global minimizer, and this may also depend on the choice of the initialization of the algorithm.

2.1.2 m levels

More levels $\{l_1 < l_2 < ... < l_m\}$ can be considered, instead of only two $\{l_1 = 0 < l_2 = l\}$. The energy in this more general case will be:

$$\inf_{c_1,c_2,...,c_{m+1},\phi} F(c_1,c_2,...,c_{m+1},\phi) =$$

$$\int_\Omega |f(x)-c_1|^2 H(l_1-\phi(x))dx$$

$$+\sum_{i=2}^{m}\int_\Omega |f(x)-c_i|^2 H(\phi(x)-l_{i-1})H(l_i-\phi(x))dx$$

$$+\int_\Omega |f(x)-c_{m+1}|^2 H(\phi(x)-l_m)dx$$

$$+\mu\sum_{i=1}^{m}\int_\Omega |\nabla H(\phi-l_i)|.$$

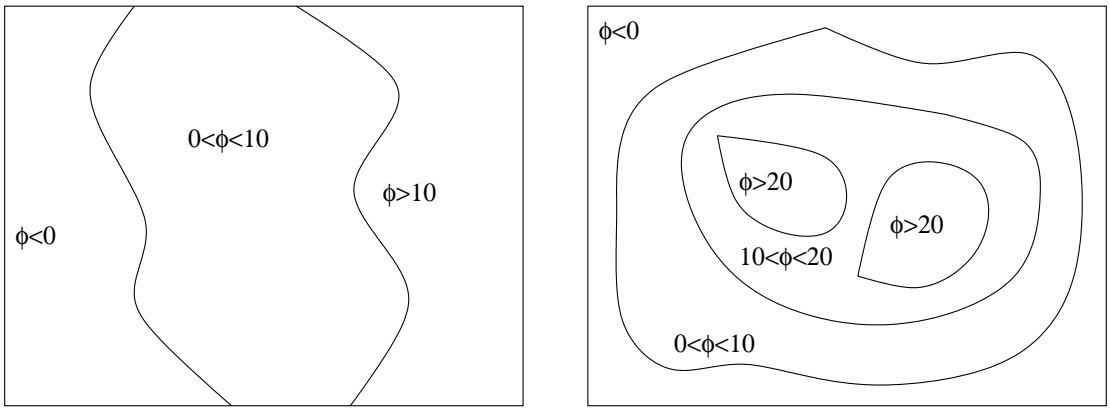

Figure 1: Left: the level lines $\{x \in \Omega : \ \phi(x) = 0\}$, $\{x \in \Omega : \ \phi(x) = 10\}$ partition the domain Ω into 3 disjoint regions. Right: the level lines $\{x \in \Omega : \ \phi(x) = 0\}$, $\{x \in \Omega : \ \phi(x) = 10\}$, $\{x \in \Omega : \ \phi(x) = 20\}$ partition the domain Ω into 4 disjoint regions.

The associated Euler-Lagrange equations in this more general case, can be expressed in a similar way, as follows: in a dynamical scheme, starting with $\phi(0, x) = \phi_0(x)$, solve for $t > 0$

$$\begin{aligned} c_1(t) &= \frac{\int_\Omega f(x) H(l_1 - \phi(t,x)) dx}{\int_\Omega H(l_1 - \phi(t,x)) dx}, \\ c_i(t) &= \frac{\int_\Omega f(x) H(\phi(t,x) - l_{i-1}) H(l_i - \phi(t,x)) dx}{\int_\Omega H(\phi(t,x) - l_{i-1}) H(l_i - \phi(t,x)) dx}, \\ c_{m+1}(t) &= \frac{\int_\Omega f(x) H(\phi(t,x) - l_m) dx}{\int_\Omega H(\phi(t,x) - l_m) dx}, \end{aligned}$$

for $i = 2, ..., m$, and

$$\begin{aligned} \frac{\partial \phi}{\partial t} &= \delta_\varepsilon(l_1 - \phi)|f - c_1|^2 \\ &+ \sum_{i=2}^{m} \Big[- \delta_\varepsilon(\phi - l_{i-1}) H(l_i - \phi)|f - c_i|^2 \\ &+ \delta_\varepsilon(l_i - \phi) H(\phi - l_{i-1})|f - c_i|^2 \Big] \\ &- \delta_\varepsilon(\phi - l_m)|f - c_{m+1}|^2 \\ &+ \mu \sum_{i=1}^{m} \Big[\delta_\varepsilon(\phi - l_i) \mathrm{div}\Big(\frac{\nabla \phi}{|\nabla \phi|}\Big) \Big], \end{aligned}$$

together with the corresponding boundary conditions on $\partial\Omega$, for $t > 0$.

We show in Figure 1 examples of partitions of the domain Ω, using two and three level lines of a Lipschitz continuous function ϕ.

2.1.3 Experimental results

We show in this section experimental results applied to synthetic and real images. In each figure, we show the evolution over time of the segmented image u of averages (left column),

and the evolving set of curves superposed over the initial image f (right column). We also give the main parameters used in the calculations and the CPU times, together with the evolution of the energy versus iterations. We have used here a finite differences semi-implicit numerical discretization, and the details are given in the Appendix.

In Figures 2-4, we illustrate how the model works on synthetic images (including noisy images), in the case $m = 3$, where m is the number of the nested level lines of the function ϕ used to partition the domain Ω. In Figure 2 we illustrate both the segmentation and denoising properties of the model, while in Figures 3 and 4 we illustrate the change of topology.

In Figures 5-6, we illustrate how the models work on real noisy images of poor resolution, representing blood cells. Here, the model with two level lines of the function ϕ has been applied, producing very satisfactory results. In Fig. 7, application to brain data segmentation is illustrated.

We note that in all these cases, in the piecewise-constant segmentation models from [32], [33], and [35], we would have needed more than one function ϕ for the segmentation, therefore more computational storage is required. In practice, we do not impose that ϕ is Lipschitz continuous. The parameter levels l_1, l_2, ... are here kept constant and fixed for all our different experimental calculations. These can also be specified by the user. We have not implemented an automatic procedure of selection of these parameter levels. Sometimes, these could be estimated if a statistical prior exists about the contours or level lines of the data. We note that the algorithm is not sensitive with respect to the change of these parameter levels l_i. As in the model from [35], only an upper bound of the phases is needed. For instance we can segment an image into 2 regions, using the model with one level set function and 2 levels (therefore with 3 regions in theory, but only two regions will appear in practice). Note that in all cases, the energy reaches a minimum (local or global) very fast, only after a small number of iterations. The only varying parameter in this set of results is the coefficient of the length term, which has a scaling role. Note that in Fig. 3, during the evolution, two distinct level lines of the same function ϕ can become very close in position, almost like for a triple junction, but without overlap.

2.2 The case of two functions

As in [35], we can extend the multilayer model from the previous section to the case of more than one level set function. This may be needed for instance for images with triple junctions and with more complex structure. Here, we will use only two level set functions, to represent up to nine distinct regions of different intensities, making up Ω. We will work with the functions ϕ_1 and ϕ_2, and with two levels $\{0,\ l\}$, with $l > 0$.

The nine regions defined by the two level set functions and two levels are:

$$\begin{aligned} R_{11} &= \{x \in \Omega :\ \phi_1 < 0,\ \phi_2 < 0\}, \\ R_{21} &= \{x \in \Omega :\ 0 < \phi_1 < l,\ \phi_2 < 0\}, \\ R_{31} &= \{x \in \Omega :\ \phi_1 > l,\ \phi_2 < 0\}, \\ R_{12} &= \{x \in \Omega :\ \phi_1 < 0,\ 0 < \phi_2 < l\}, \end{aligned}$$

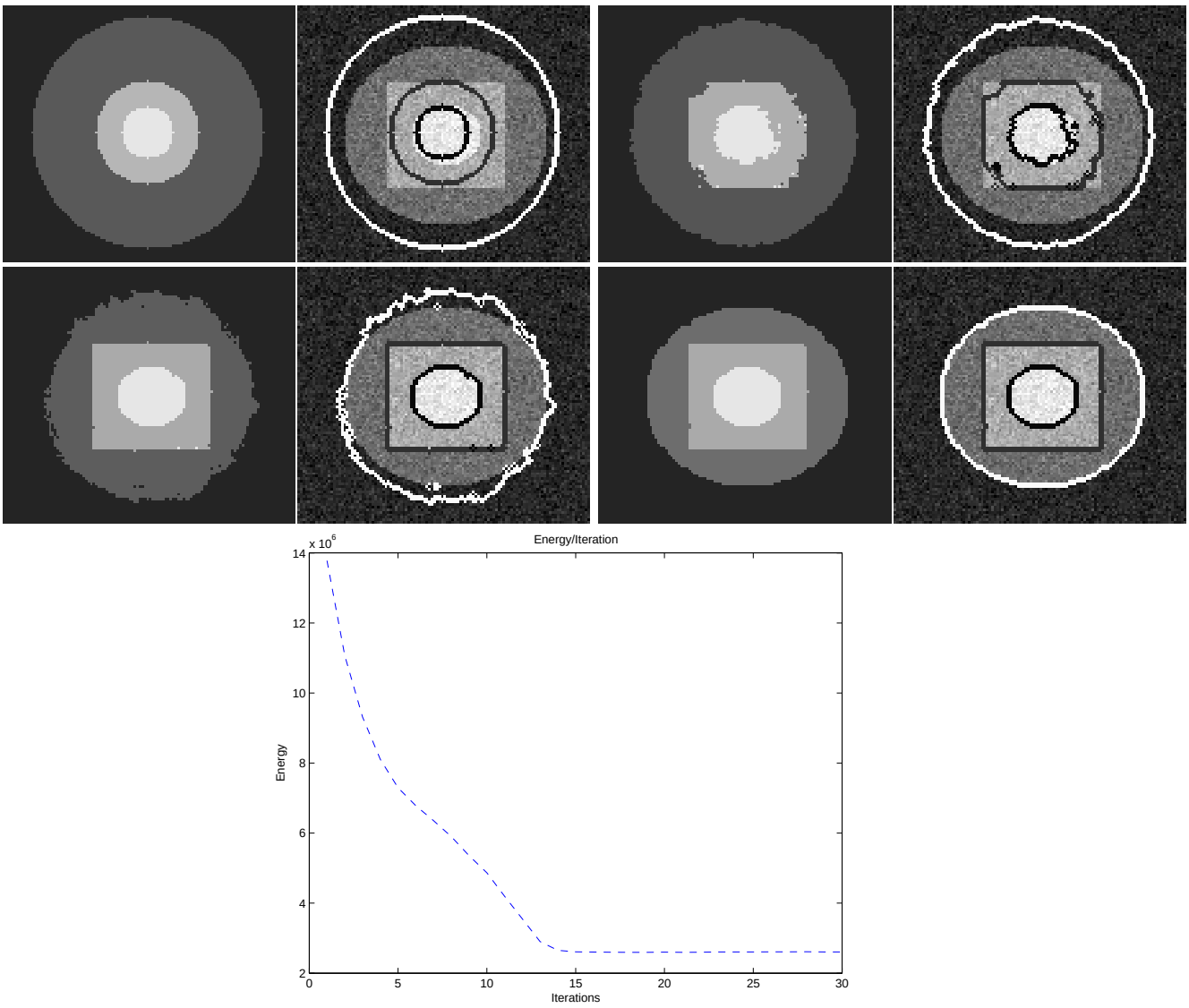

Figure 2: Segmentation of a noisy synthetic image using one level set function ϕ and 3 levels. Parameters: $l_1 = 0$, $l_2 = 25$, $l_3 = 35$, $\triangle t = 0.1$, $\mu = 0.0217 * 255^2$, 30 iterations, cpu time 0.41 sec.

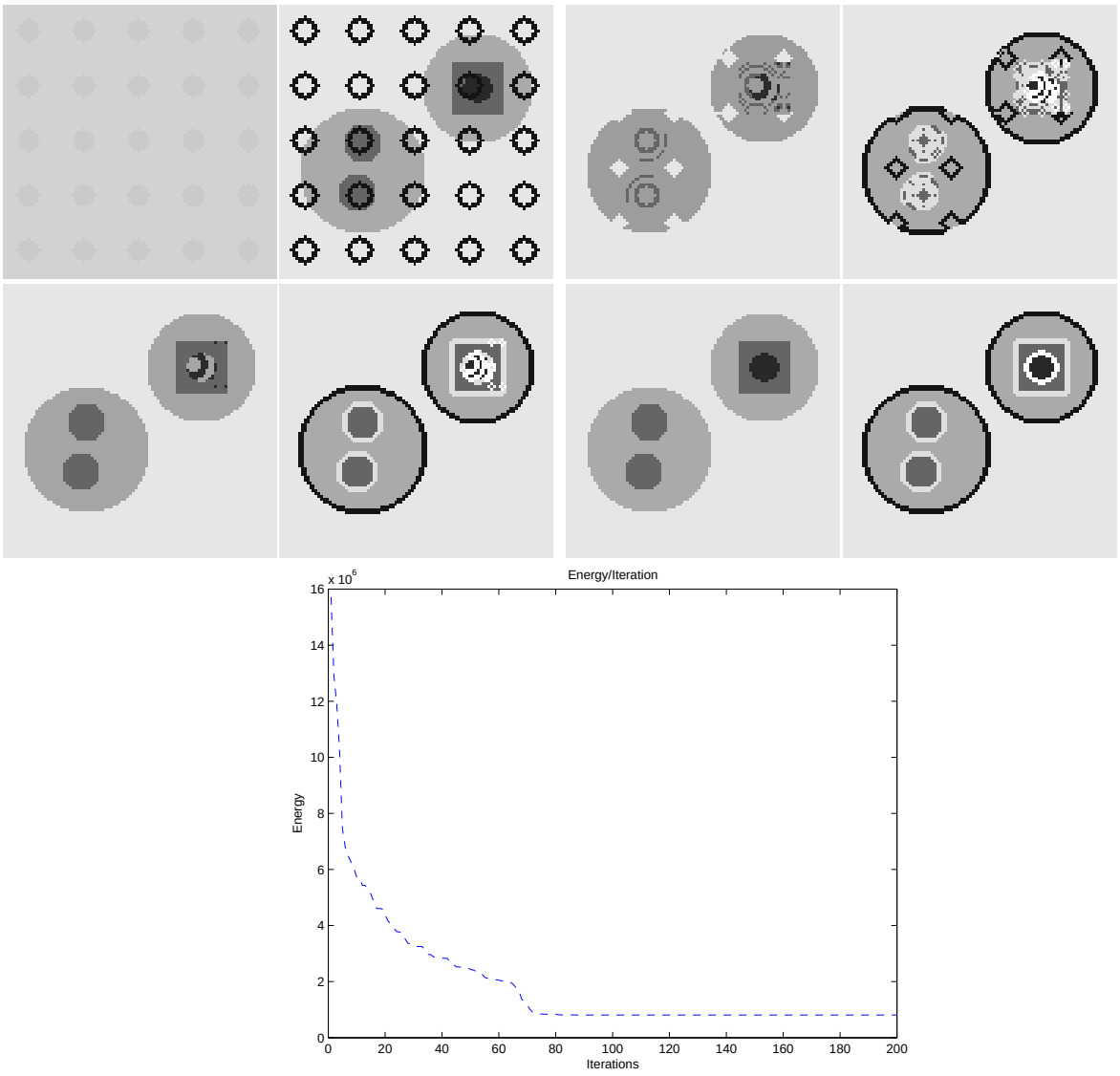

Figure 3: Segmentation of a synthetic image of several objects with a nested structure, using one level set function ϕ and 3 levels. Parameters: $l_1 = 0$, $l_2 = 25$, $l_3 = 35$, $\triangle t = 0.1$, $\mu = 0.0000511 * 255^2$, 200 iterations, cpu time 4.015 sec.

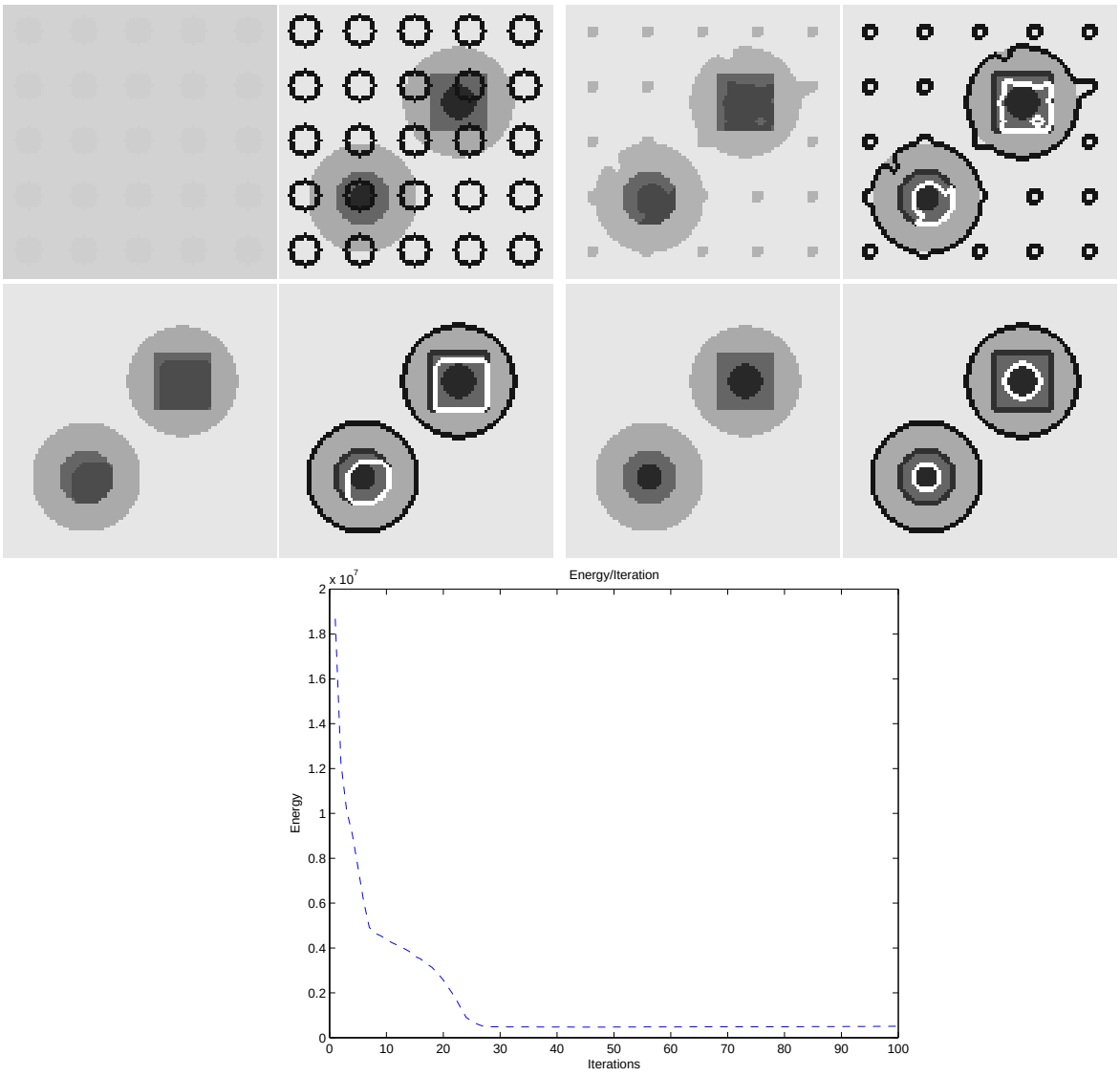

Figure 4: Segmentation of a synthetic image of several objects with a nested structure, using one level set function ϕ and 3 levels. Parameters: $l_1 = 0$, $l_2 = 25$, $l_3 = 35$, $\triangle t = 0.1$, $\mu = 0.0101 * 255^2$, 100 iterations, cpu time 1.586 sec.

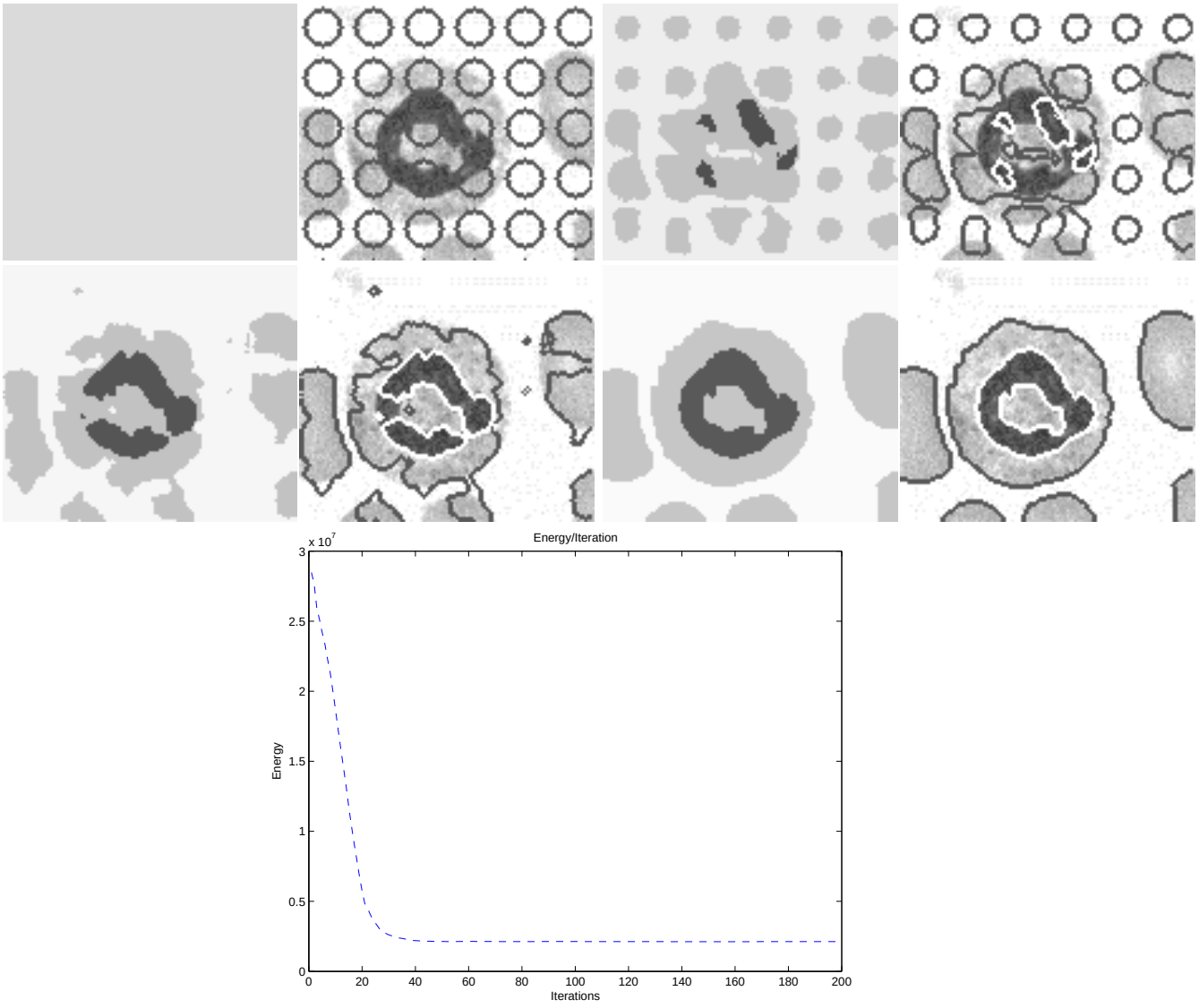

Figure 5: Segmentation of a noisy real blood cells image using one level set function and two levels. Parameters: $l_1 = 0$, $l_2 = 25$, $\triangle t = 0.1$, $\mu = 0.03 * 255^2$, 200 iterations, cpu time 2.51 sec.

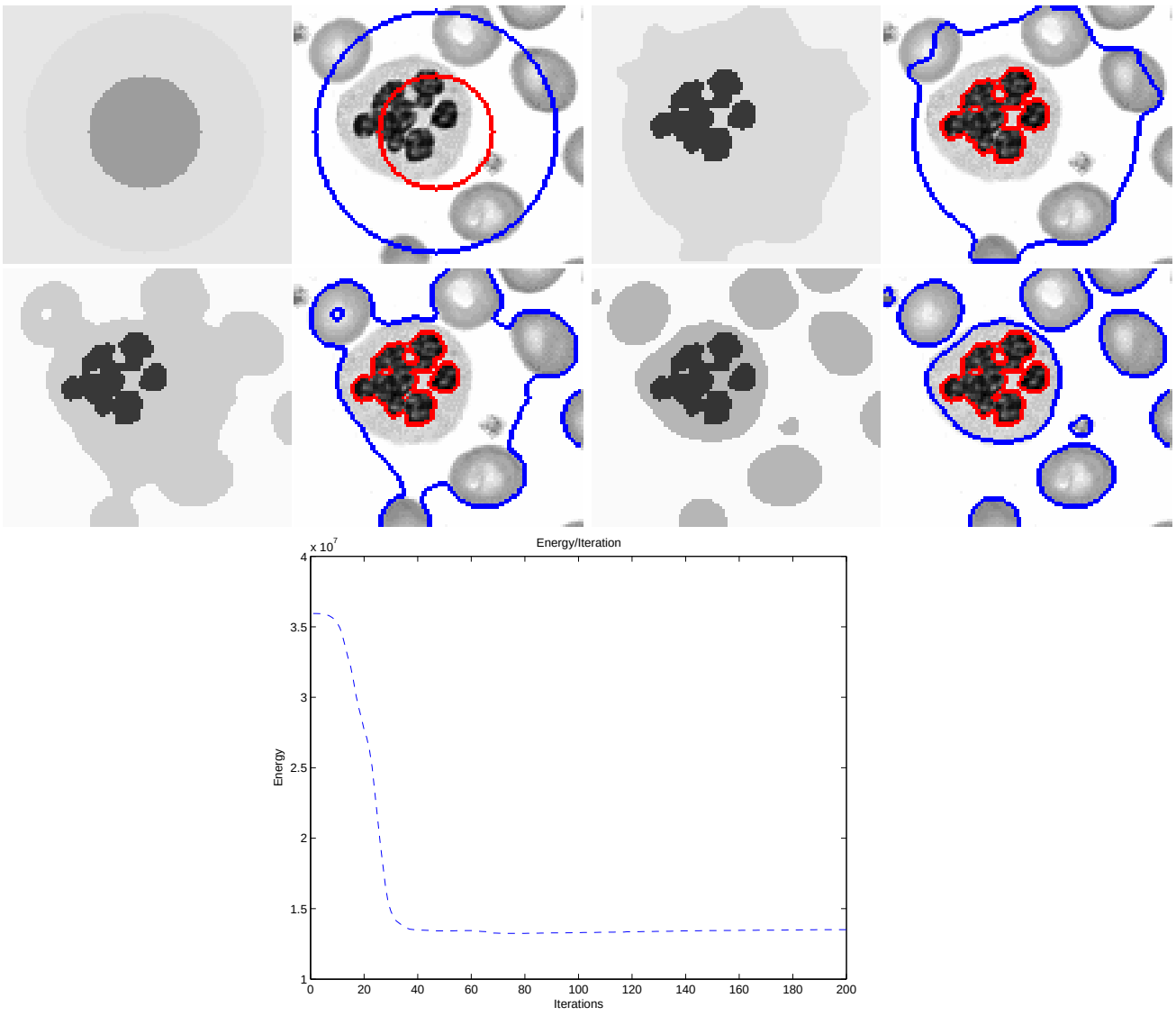

Figure 6: Segmentation of another noisy real blood cells image using one level set function and two levels. Parameters: $l_1 = 0$, $l_2 = 25$, $\triangle t = 0.1$, $\mu = 0.043 * 255^2$, 200 iterations, cpu time 2.493 sec.

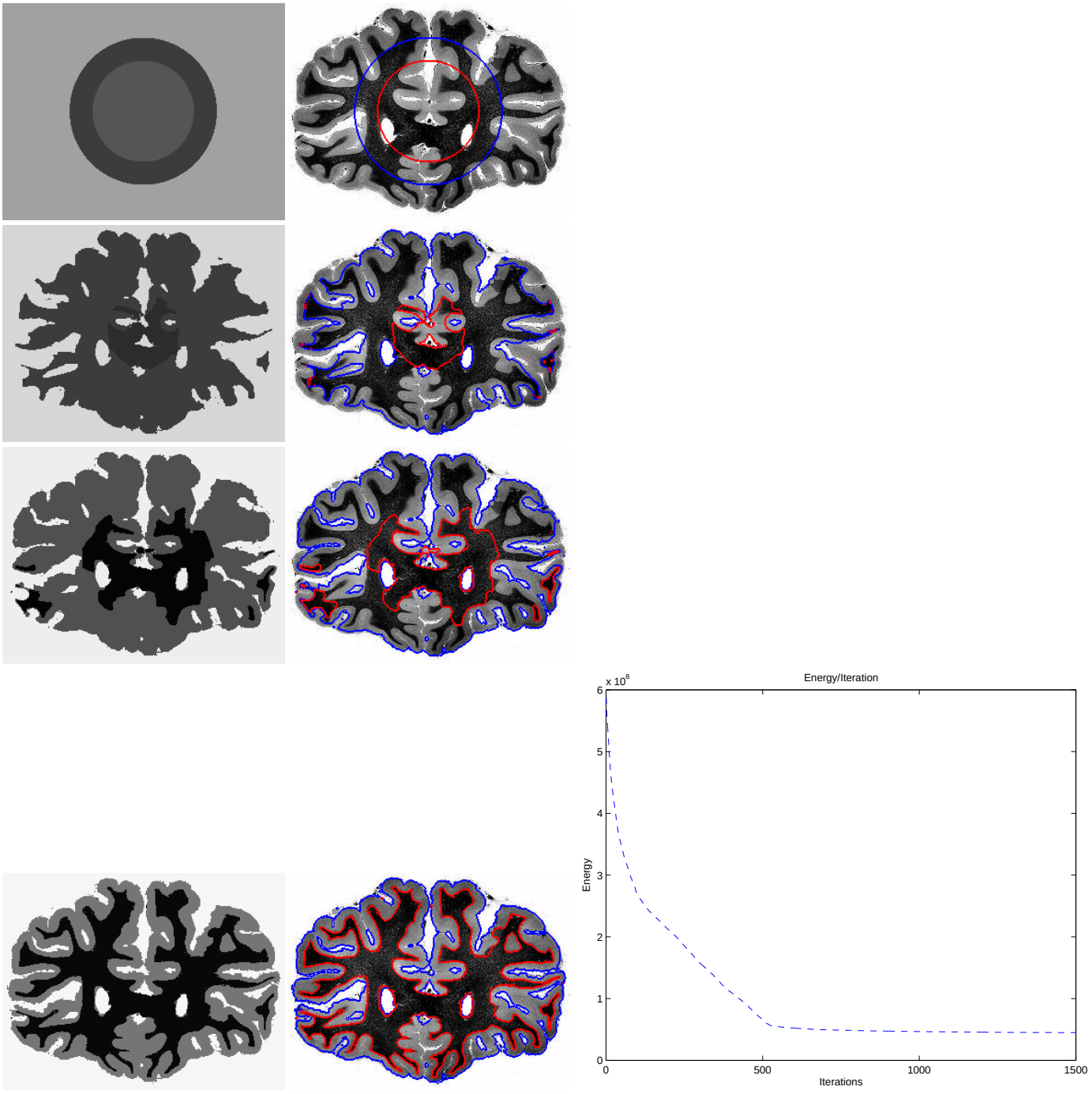

Figure 7: Segmentation of a brain image using one level set function with two levels. Parameters: $l_1 = 0$, $l_2 = 25$, $\triangle t = 0.1$, $\mu = 0.1 * 255^2$, 1500 iterations, cpu time 183.544 sec.

$$
\begin{aligned}
R_{22} &= \{x \in \Omega :\ 0 < \phi_1 < l,\ 0 < \phi_2 < l\},\\
R_{32} &= \{x \in \Omega :\ \phi_1 > l,\ 0 < \phi_2 < l\},\\
R_{13} &= \{x \in \Omega :\ \phi_1 < 0,\ \phi_2 > l\},\\
R_{23} &= \{x \in \Omega :\ 0 < \phi_1 < l,\ \phi_2 > l\},\\
R_{33} &= \{x \in \Omega :\ \phi_1 > l,\ \phi_2 > l\}.
\end{aligned}
$$

Following the previous section and [35], the associated energy for image segmentation is:

$$
\begin{aligned}
\inf_{\vec{c},\Phi} F(\vec{c},\Phi) = \int_\Omega \Big[& |f(x)-c_{11}|^2 H(-\phi_1(x))H(-\phi_2(x))\\
& + |f(x)-c_{21}|^2 H(\phi_1(x))H(l-\phi_1(x))H(-\phi_2(x))\\
& + |f(x)-c_{31}|^2 H(\phi_1(x)-l)H(-\phi_2(x))\\
& + |f(x)-c_{12}|^2 H(-\phi_1(x))H(\phi_2(x))H(l-\phi_2(x))\\
& + |f(x)-c_{22}|^2 H(\phi_1(x))H(l-\phi_1(x))H(\phi_2(x))H(l-\phi_2(x))\\
& + |f(x)-c_{32}|^2 H(\phi_1(x)-l)H(\phi_2(x))H(l-\phi_2(x))\\
& + |f(x)-c_{13}|^2 H(-\phi_1(x))H(\phi_2(x)-l)\\
& + |f(x)-c_{23}|^2 H(\phi_1(x))H(l-\phi_1(x))H(\phi_2(x)-l)\\
& + |f(x)-c_{33}|^2 H(\phi_1(x)-l)H(\phi_2(x)-l)\Big]dx\\
& + \mu\Big[\int_\Omega |\nabla H(\phi_1)| + \int_\Omega |\nabla H(\phi_1-l)|\\
& + \int_\Omega |\nabla H(\phi_2)| + \int_\Omega |\nabla H(\phi_2-l)|\Big],
\end{aligned}
$$

where $\vec{c} = (c_{11}, c_{21}, c_{31}, c_{12}, c_{22}, c_{32}, c_{13}, c_{23}, c_{33})$ is the unknown vector of averages, and $\Phi = (\phi_1, \phi_2)$ is a vector-valued unknown function.

Embedding the minimization in a dynamical scheme, and starting with $\phi_1(0,x) = \phi_{1,0}(x)$ and $\phi_2(0,x) = \phi_{2,0}(x)$, we have that the unknown constants $c_{11}, c_{21}, ...$ are given by the averages of the data f on their corresponding regions $R_{11}, R_{21}, ...$, as follows:

$$
\begin{aligned}
c_{11}(t) &= \frac{\int_\Omega f H(-\phi_1)H(-\phi_2)dx}{\int_\Omega H(-\phi_1)H(-\phi_2)dx},\\
c_{21}(t) &= \frac{\int_\Omega f H(\phi_1)H(l-\phi_1)H(-\phi_2)dx}{\int_\Omega H(\phi_1)H(l-\phi_1)H(-\phi_2)dx},\\
c_{31}(t) &= \frac{\int_\Omega f H(\phi_1-l)H(-\phi_2)dx}{\int_\Omega H(\phi_1-l)H(-\phi_2)dx},\\
c_{12}(t) &= \frac{\int_\Omega f H(-\phi_1)H(\phi_2)H(l-\phi_2)dx}{\int_\Omega H(-\phi_1)H(\phi_2)H(l-\phi_2)dx},\\
c_{22}(t) &= \frac{\int_\Omega f H(\phi_1)H(\phi_2)H(l-\phi_1)H(l-\phi_2)dx}{\int_\Omega H(\phi_1)H(\phi_2)H(l-\phi_1)H(l-\phi_2)dx},\\
c_{32}(t) &= \frac{\int_\Omega f(x) H(\phi_1-l)H(\phi_2)H(l-\phi_2)dx}{\int_\Omega H(\phi_1-l)H(\phi_2)H(l-\phi_2)dx},
\end{aligned}
$$

$$
\begin{aligned}
c_{13}(t) &= \frac{\int_\Omega f H(-\phi_1)H(\phi_2-l)dx}{\int_\Omega H(-\phi_1)H(\phi_2-l)dx},\\
c_{23}(t) &= \frac{\int_\Omega f H(\phi_1)H(l-\phi_1)H(\phi_2-l)dx}{\int_\Omega H(\phi_1)H(l-\phi_1)H(\phi_2-l)dx},\\
c_{33}(t) &= \frac{\int_\Omega f H(\phi_1-l)H(\phi_2-l)dx}{\int_\Omega H(\phi_1-l)H(\phi_2-l)dx}.
\end{aligned}
$$

The unknown functions ϕ_1 and ϕ_2 are solutions of the following equations:

$$
\begin{aligned}
\phi_1(0,x) &= \phi_{1,0}(x),\\
\phi_2(0,x) &= \phi_{2,0}(x),\\
\frac{\partial\phi_1}{\partial t} &= \delta_\varepsilon(\phi_1)\Big[|f-c_{11}|^2H(-\phi_2)\\
&-|f-c_{21}|^2H(l-\phi_1)H(-\phi_2)+|f-c_{12}|^2H(\phi_2)H(l-\phi_2)\\
&-|f-c_{22}|^2H(l-\phi_1)H(\phi_2)H(l-\phi_2)\\
&+|f-c_{13}|^2H(\phi_2-l)-|f-c_{23}|^2H(l-\phi_1)H(\phi_2-l)\\
&+\mu\mathrm{div}\Big(\frac{\nabla\phi_1}{|\nabla\phi_1|}\Big)\Big]\\
&+\delta_\varepsilon(\phi_1-l)\Big[|f-c_{21}|^2H(\phi_1)H(-\phi_2)-|f-c_{31}|^2H(-\phi_2)\\
&+|f-c_{22}|^2H(\phi_1)H(\phi_2)H(l-\phi_2)\\
&-|f-c_{32}|^2H(\phi_2)H(l-\phi_2)\\
&+|f-c_{23}|^2H(\phi_1)H(\phi_2-l)-|f-c_{33}|^2H(\phi_2-l)\\
&+\mu\mathrm{div}\Big(\frac{\nabla\phi_1}{|\nabla\phi_1|}\Big)\Big],\\
\frac{\partial\phi_2}{\partial t} &= \delta_\varepsilon(\phi_2)\Big[|f-c_{11}|^2H(-\phi_1)\\
&-|f-c_{12}|^2H(-\phi_1)H(l-\phi_2)+|f-c_{21}|^2H(\phi_1)H(l-\phi_1)\\
&-|f-c_{22}|^2H(\phi_1)H(l-\phi_1)H(l-\phi_2)\\
&+|f-c_{31}|^2H(\phi_1-l)-|f-c_{32}|^2H(\phi_1-l)H(l-\phi_2)\\
&+\mu\mathrm{div}\Big(\frac{\nabla\phi_2}{|\nabla\phi_2|}\Big)\Big]\\
&+\delta_\varepsilon(\phi_2-l)\Big[|f-c_{12}|^2H(-\phi_1)H(\phi_2)-|f-c_{13}|^2H(-\phi_1)\\
&+|f-c_{22}|^2H(\phi_1)H(l-\phi_1)H(\phi_2)\\
&-|f-c_{23}|^2H(\phi_1)H(l-\phi_1)\\
&+|f-c_{32}|^2H(\phi_1-l)H(\phi_2)-|f-c_{33}|^2H(\phi_1-l)\\
&+\mu\mathrm{div}\Big(\frac{\nabla\phi_2}{|\nabla\phi_2|}\Big)\Big].
\end{aligned}
$$

We show in Figure 8 an example of partition of the domain Ω, using two level lines corresponding to $l_1 = 0$, $l_2 = 10$, and two continuous functions ϕ_1, ϕ_2.

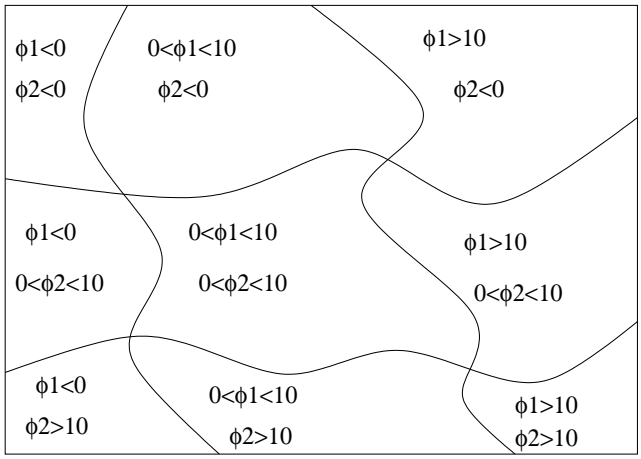

Figure 8: The level lines $\{x \in \Omega : \ \phi_i(x) = 0\}$ and $\{x \in \Omega : \ \phi_i(x) = 10\}$, $i = 1, 2$, partition the domain Ω into 9 disjoint regions.

The corresponding theoretical results can be obtained in the same way as in the previous section. Note that, as in the multi-phase models from [35] and [36], when two level set functions are used to represent the contours, as in this subsection, then it is possible that two level lines of the different functions ϕ_1 and ϕ_2 may partially overlap, and therefore by the above formulation the length of the common contour will be counted more than once and will have a different weight. This is different from the Mumford and Shah energy [26]. This is not a problem in practice, as seen in the numerical approximations. Moreover, this can also be simply avoided, as explained in [36].

We show next a few experimental results using this case, where only two level set functions ϕ_1, ϕ_2 are used, to represent up to nine disjoint regions, making up Ω.

2.2.1 Experimental results and comparisons

We show now numerical results on images with junctions, using our proposed new model with two functions ϕ_1, ϕ_2 and two levels.

We present in Figure 9 a numerical result of segmentation and partition of a noisy synthetic image, composed of 5 regions of distinct intensities. All regions and corresponding intensities are correctly detected and represented. The model uses 9 phases in theory, but at steady state only 5 appear. We also present in Fig. 10 a comparison with the multi-phase model introduced in [35]. Note that the new multilayer model reaches faster the steady state, only after 40 iterations. By the previous model [35], the energy has not yet reached a steady state after 300 iterations. The CPU time comparison shows that the new model produces faster results. There is no difference in the quality of the segmentation (the RMSE's are practically the same) between the two models.

In Figure 11 we present numerical results obtained for segmentation and partition of another blood cell image. In Figure 12 we have a numerical result of a noisy synthetic color image consisting of 9 regions of distinct intensities.

We note again that in Fig. 2 the following situation appeared: two level lines of the same

level set function became very close in position, almost like for a triple junction, but these cannot overlap.

Appendix

Energy decrease We assume here that the differentiation under the integral sign can be done and that the functions that appear are sufficiently smooth (possibly by substituting H, δ by $H_\varepsilon, \delta_\varepsilon$), so that the differentiations and all integrals are well defined.

Theorem 1: *If $(c_1(t), c_2(t), c_3(t), \phi(t,\cdot))$ satisfies the system of equations (3)-(8), for a given initial data ϕ_0 and $t \geq 0$, then $t \mapsto F_\varepsilon(c_1(t), c_2(t), c_3(t), \phi(t,\cdot))$ is decreasing.*

Proof. We formally have

$$\begin{aligned}
&\frac{d}{dt}F(c_1(t), c_2(t), c_3(t), \phi(t,\cdot)) = \\
&-\int_\Omega 2|f-c_1(t)|c_1'(t)H(-\phi)dx - \int_\Omega |f-c_1(t)|^2\delta(\phi)\phi_t dx \\
&-\int_\Omega 2|f-c_2(t)|c_2'(t)H(\phi)H(l-\phi)dx \\
&+\int_\Omega |f-c_2(t)|^2\delta(\phi)\phi_t H(l-\phi)dx \\
&-\int_\Omega |f-c_2(t)|^2\delta(\phi-l)\phi_t H(\phi)dx \\
&-\int_\Omega 2|f-c_3(t)|c_3'(t)H(\phi-l)dx \\
&+\int_\Omega |f-c_3(t)|^2\delta(\phi-l)\phi_t dx \\
&+\int_\Omega \delta'(\phi)\phi_t|\nabla\phi|dx + \int_\Omega \delta(\phi)\frac{\nabla\phi\nabla\phi_t}{|\nabla\phi|}dx \\
&+\int_\Omega \delta'(\phi-l)\phi_t|\nabla\phi|dx + \int_\Omega \delta(\phi-l)\frac{\nabla\phi\nabla\phi_t}{|\nabla\phi|}dx.
\end{aligned}$$

We note that $\int_\Omega |f-c_1(t)|H(-\phi)dx = 0$, $\int_\Omega |f-c_2(t)|H(\phi)H(l-\phi)dx = 0$, and $\int_\Omega |f-c_3(t)|H(\phi-l)dx = 0$ by definition of c_1, c_2, and c_3. Therefore,

$$\begin{aligned}
&\frac{d}{dt}F(c_1(t), c_2(t), c_3(t), \phi(t,\cdot)) \\
=\ &\int_\Omega \delta(\phi)\phi_t\Big(-|f-c_1(t)|^2 + |f-c_2(t)|^2H(l-\phi)\Big)dx \\
+\ &\int_\Omega \delta(\phi-l)\phi_t\Big(-|f-c_2(t)|^2H(\phi) + |f-c_3(t)|^2\Big)dx \\
+\ &\int_\Omega \delta'(\phi)\phi_t|\nabla\phi|dx + \int_\Omega \delta(\phi)\frac{\nabla\phi\nabla\phi_t}{|\nabla\phi|}dx \\
+\ &\int_\Omega \delta'(\phi-l)\phi_t|\nabla\phi|dx + \int_\Omega \delta(\phi-l)\frac{\nabla\phi\nabla\phi_t}{|\nabla\phi|}dx.
\end{aligned}$$

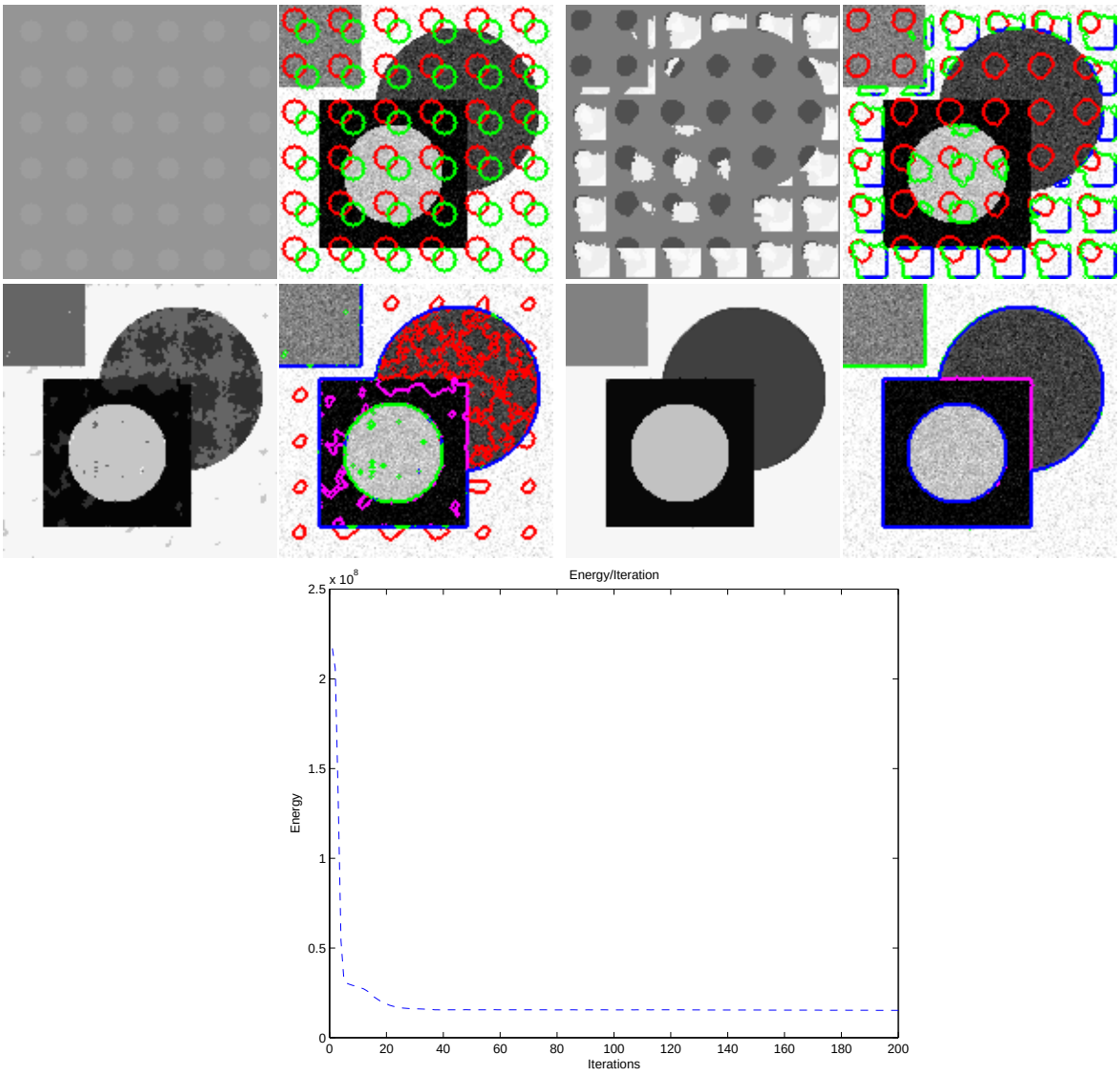

Figure 9: Segmentation of a noisy synthetic image with triple junctions, using two functions ϕ_1, ϕ_2 and two levels. Parameters: $l_1 = 0$, $l_2 = 25$, $\triangle t = 0.4$, $\mu = 0.023 * 255^2$, 200 iterations, cpu time 13.985 sec, RMSE=52.3226.

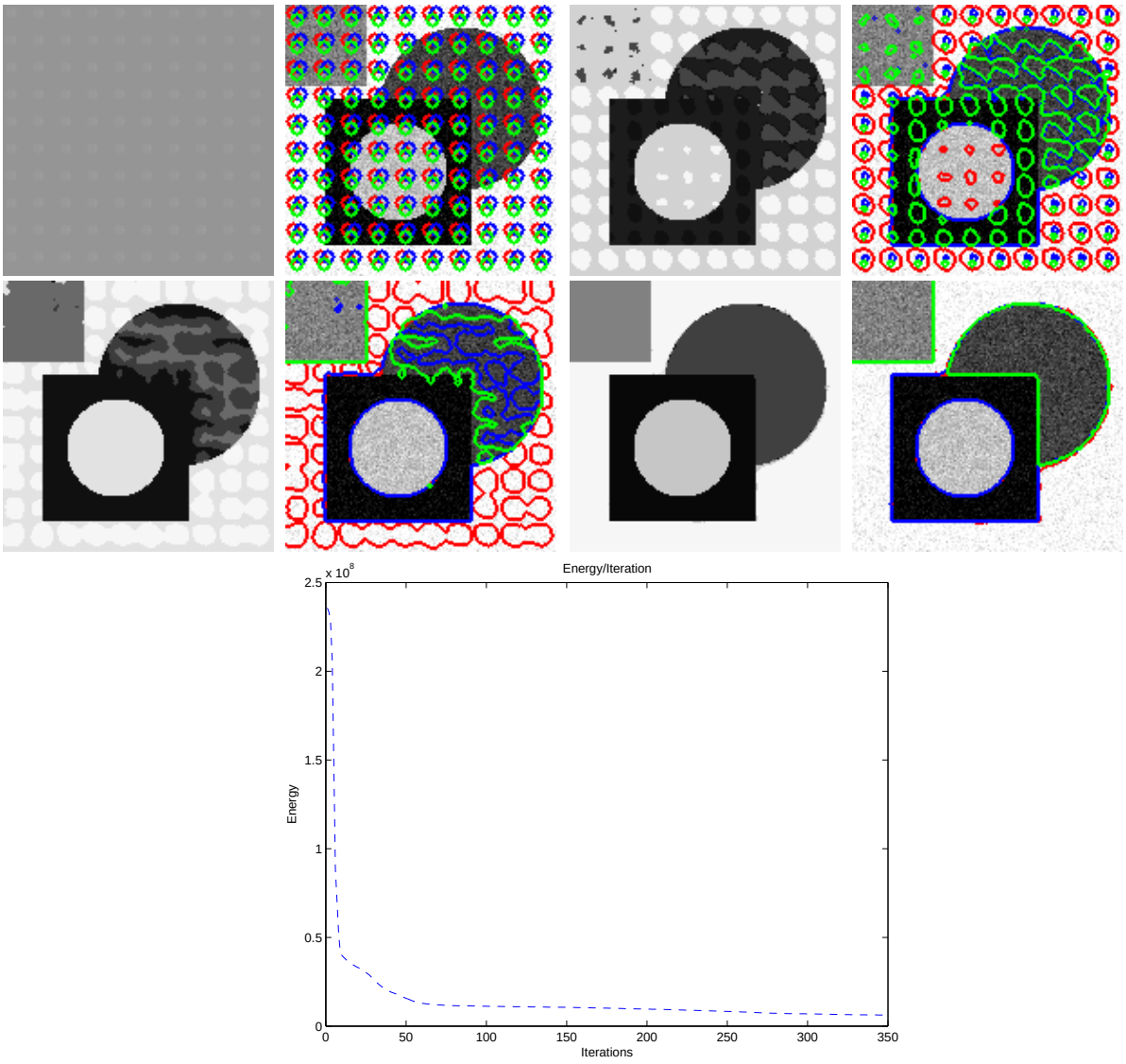

Figure 10: Segmentation obtained using the model from [35], using 3 level set functions (8 phases), each zero-level-line of ϕ_i representing a curve. Parameters: $l = 0$, $\triangle t = 0.4$, $\mu = 0.06 * 255^2$, 350 iterations, cpu time 30.967 sec, RMSE=52.70172.

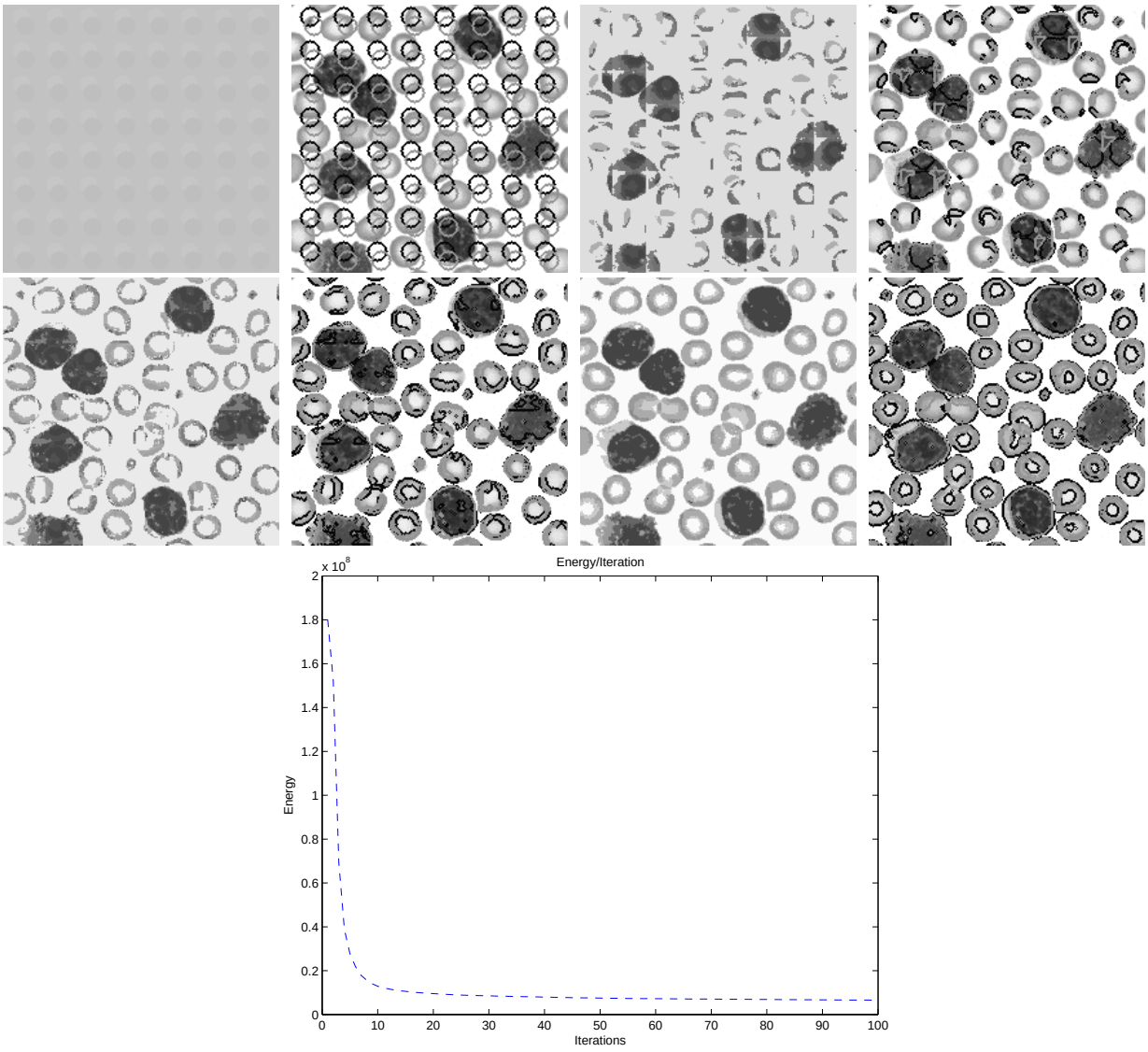

Figure 11: Segmentation of a real blood cells image with junctions, using two functions ϕ_1, ϕ_2 and two levels. Parameters: $l_1 = 0$, $l_2 = 25$, $\triangle t = 0.4$, $\mu = 0.05 * 255^2$, 100 iterations, cpu time 10.814 sec.

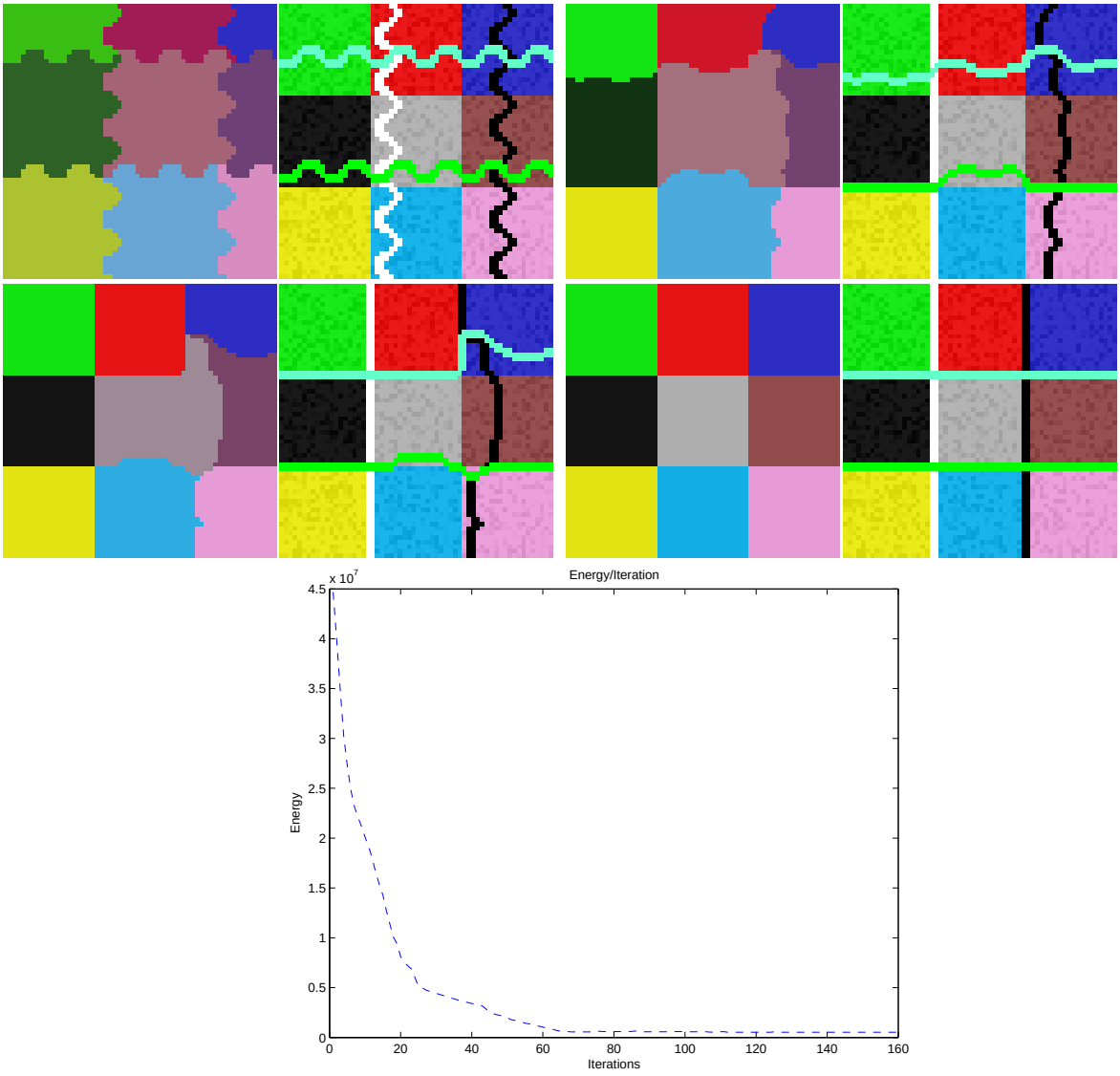

Figure 12: Segmentation of a noisy synthetic color image with junctions, using two functions ϕ_1, ϕ_2 and two levels. Parameters: $l_1 = 0$, $l_2 = 25$, $\triangle t = 0.01$, $\mu = 0.335 * 255^2$, 160 iterations, cpu time 10.975 sec. Note that the image contains nine different regions, all correctly detected and segmented in an efficient approach.

Note also that

$$\begin{aligned}\int_\Omega \delta'(\phi)\phi_t|\nabla\phi|dx + \int_\Omega \delta(\phi)\frac{\nabla\phi\nabla\phi_t}{|\nabla\phi|}dx \\ = -\int_\Omega \delta(\phi)\phi_t \mathrm{div}(\frac{\nabla\phi}{|\nabla\phi|})dx. \\ \int_\Omega \delta'(\phi-l)\phi_t|\nabla\phi|dx + \int_\Omega \delta(\phi-l)\frac{\nabla\phi\nabla\phi_t}{|\nabla\phi|}dx \\ = -\int_\Omega \delta(\phi-l)\phi_t \mathrm{div}(\frac{\nabla\phi}{|\nabla\phi|})dx.\end{aligned}$$

Then,

$$\begin{aligned}&\frac{d}{dt}F(c_1(t),c_2(t),c_3(t),\phi(t,\cdot)) \\ =\ &\int_\Omega \delta(\phi)\phi_t\Big(-|f-c_1(t)|^2+|f-c_2(t)|^2H(l-\phi)\Big)dx \\ +\ &\int_\Omega \delta(\phi-l)\phi_t\Big(-|f-c_2(t)|^2H(\phi)+|f-c_3(t)|^2\Big)dx \\ -\ &\int_\Omega \delta(\phi)\phi_t\mathrm{div}(\frac{\nabla\phi}{|\nabla\phi|})dx - \int_\Omega \delta(\phi-l)\phi_t\mathrm{div}(\frac{\nabla\phi}{|\nabla\phi|})dx.\end{aligned}$$

Let

$$\begin{aligned}A &= |f-c_1(t)|^2 - |f-c_2(t)|^2H(l-\phi), \\ B &= H(\phi)|f-c_2(t)|^2 - |f-c_3(t)|^2, \\ K &= \mathrm{div}(\frac{\nabla\phi}{|\nabla\phi|}).\end{aligned}$$

Then $\phi_t = \delta(\phi)(A+K) + \delta(\phi-l)(B+K)$, and

$$\begin{aligned}&\frac{d}{dt}F(c_1(t),c_2(t),c_3(t),\phi(t,\cdot)) \\ =\ &-\int_\Omega A\delta(\phi)\Big[\delta(\phi)(A+K)+\delta(\phi-l)(B+k)\Big]dx \\ -\ &\int_\Omega B\delta(\phi-l)\Big[\delta(\phi)(A+K)+\delta(\phi-l)(B+K)\Big]dx \\ -\ &\int_\Omega K\delta(\phi)\Big[\delta(\phi)(A+K)+\delta(\phi-l)(B+K)\Big]dx \\ -\ &\int_\Omega K\delta(\phi-l)\Big[\delta(\phi)(A+K)+\delta(\phi-l)(B+K)\Big]dx,\end{aligned}$$

$$\frac{d}{dt}F(c_1(t),c_2(t),c_3(t),\phi(t,\cdot))$$

$$
\begin{aligned}
&= -\int_\Omega \delta^2(\phi)(A+k)^2dx - \int_\Omega \delta^2(\phi-l)(B+K)^2dx \\
&- 2\int_\Omega \delta(\phi)\delta(\phi-l)(AB+AK+BK+K^2)dx \\
&= -\int_\Omega \Big(\delta^2(\phi)(A+K)^2 + \delta^2(\phi-l)(B+K)^2 \\
&+ 2\delta(\phi)\delta(\phi-l)(A+K)(B+K)\Big)dx \\
&= -\int_\Omega \Big(\delta(\phi)(A+K) + \delta(\phi-l)(B+K)\Big)^2 dx \leq 0.
\end{aligned}
$$

Description of the numerical algorithm Let h be the space step, $\triangle t$ be the time step, and $\varepsilon = h$. Let (x_i, y_j) be the discrete points, for $1 \leq i, j \leq M$, and $f_{i,j} \approx f(x_i, y_j)$, $\phi^n_{i,j} \approx \phi(n\triangle t, x_i, y_j)$, with $n \geq 0$. We present the details of the numerical algorithm for the case of one function with two levels given in (3)-(8). Set $n = 0$, and start with $\phi^0_{i,j}$ given (defining the initial set of curves). Then, for each $n > 0$ until steady state:

1) compute the averages $c^n_1 \approx c_1(n\triangle t)$, $c^n_2 \approx c_2(n\triangle t)$, and $c^n_3 \approx c_3(n\triangle t)$.

2) compute $\phi^{n+1}_{i,j}$, derived from the finite differences scheme:

$$
\begin{aligned}
\frac{\phi^{n+1}_{i,j} - \phi^n_{i,j}}{\triangle t} = \delta_\varepsilon(\phi^n_{i,j})\Big[\frac{\mu}{h^2}\Big(\triangle^x_-\Big(\frac{\phi^n_{i+1,j} - \phi^{n+1}_{i,j}}{|\nabla\phi^n_{i,j}|}\Big) \\
+\triangle^y_-\Big(\frac{\phi^n_{i,j+1} - \phi^{n+1}_{i,j}}{|\nabla\phi^n_{i,j}|}\Big)\Big) \\
+|f_{i,j} - c^n_1|^2 - |f_{i,j} - c^n_2|^2 H_\varepsilon(l - \phi^n_{i,j})\Big] \\
+\delta_\varepsilon(\phi^n_{i,j} - l)\Big[\frac{\mu}{h^2}\Big(\triangle^x_-\Big(\frac{\phi^n_{i+1,j} - \phi^{n+1}_{i,j}}{|\nabla phi^n_{i,j}|}\Big) \\
+\triangle^y_-\Big(\frac{\phi^n_{i,j+1} - \phi^{n+1}_{i,j}}{|\nabla phi^n_{i,j}|}\Big)\Big) \\
-|f_{i,j} - c^n_3|^2 + |f_{i,j} - c^n_2|^2 H_\varepsilon(\phi^n_{i,j})\Big].
\end{aligned}
$$

Let

$$
\begin{aligned}
C_1 &= \frac{1}{\sqrt{\Big(\frac{\phi^n_{i+1,j} - \phi^n_{i,j}}{h}\Big)^2 + \Big(\frac{\phi^n_{i,j+1} - \phi^n_{i,j-1}}{2h}\Big)^2}}, \\
C_2 &= \frac{1}{\sqrt{\Big(\frac{\phi^n_{i,j} - \phi^n_{i-1,j}}{h}\Big)^2 + \Big(\frac{\phi^n_{i-1,j+1} - \phi^n_{i-1,j-1}}{2h}\Big)^2}}, \\
C_3 &= \frac{1}{\sqrt{\Big(\frac{\phi^n_{i+1,j} - \phi^n_{i-1,j}}{2h}\Big)^2 + \Big(\frac{\phi^n_{i,j+1} - \phi^n_{i,j}}{h}\Big)^2}}, \\
C_4 &= \frac{1}{\sqrt{\Big(\frac{\phi^n_{i+1,j-1} - \phi^n_{i-1,j-1}}{2h}\Big)^2 + \Big(\frac{\phi^n_{i,j} - \phi^n_{i,j-1}}{h}\Big)^2}}.
\end{aligned}
$$

Let $m_1 = \frac{\triangle t}{h^2}(\delta_\varepsilon(\phi^n_{i,j}) + \delta_\varepsilon(\phi^n_{i,j} - l))\mu$, $C = 1 + m_1(C_1 + C_2 + C_3 + C_4)$,

$$\phi^{n+1}_{i,j} = \frac{1}{C}\Big[\phi^n_{i,j} + m_1(C_1\phi^n_{i+1,j} + C_2\phi^n_{i-1,j} + C_3\phi^n_{i,j+1} + C_4\phi^n_{i,j-1}) + \triangle t\delta_\varepsilon(\phi^n_{i,j})(-(f_{i,j} - c^n_2)^2(1 - H_\varepsilon(\phi^n_{i,j} - l)) + (f_{i,j} - c^n_3)^2) + \triangle t\delta_\varepsilon(\phi^n_{i,j} - l)(-(f_{i,j} - c^n_1)^2 + (f_{i,j} - c^n_2)^2 H_\varepsilon(\phi^n_{i,j}))\Big].$$

Existence of minimizers For simplicity of notations, we show the existence of minimizers for the case of one function with two levels. Assume $f \in L^\infty(\Omega)$, that Ω is open, bounded, connected and with Lipschitz boundary $\partial\Omega$. Let us denote by $\chi_1 = H(\phi)$, $\chi_2 = H(\phi - l)$, where now χ_1 and χ_2 have to be characteristic functions of two sets E_1 and E_2, with $E_2 \subset E_1$ (this means that if $\chi_2(x) = 1$ at some point $x \in \Omega$, then $\chi_1(x) = 1$ also). This will guarantee that in the new formulation: $1 - \chi_1(x) + \chi_1(x)(1 - \chi_2(x)) + \chi_2(x) = 1$ for all $x \in \Omega$, i.e. a perfect partition.

Then the problem (2) can be reformulated as

$$\begin{aligned}\inf_{\chi_1,\chi_2} F(\chi_1,\chi_2) = &\int_\Omega (f - c_1(\chi_1))^2(1 - \chi_1)dx \\ &+ \int_\Omega (f - c_2(\chi_1,\chi_2))^2\chi_1(1 - \chi_2)dx \\ &+ \int_\Omega (f - c_3(\chi_2))^2\chi_2 dx + \mu\int_\Omega |\nabla\chi_1| + \mu\int_\Omega |\nabla\chi_2|,\end{aligned} \tag{9}$$

with $c_1(\chi_1) = \frac{\int_\Omega f(x)(1-\chi_1)dx}{\int_\Omega(1-\chi_1)dx}$, $c_2(\chi_1,\chi_2) = \frac{\int_\Omega f(x)\chi_1(1-\chi_2)dx}{\int_\Omega \chi_1(1-\chi_2)dx}$, $c_3(\chi_2) = \frac{\int_\Omega f(x)\chi_2 dx}{\int_\Omega \chi_2 dx}$.

This minimization is among characteristic functions χ_1, χ_2 of sets of finite perimeter, i.e. on the set $\Big\{\chi_i \in BV(\Omega), \chi_i(x) \in \{0,1\}$ almost everywhere, $i = 1,2\Big\}$, and such that $\chi_1 \geq \chi_2$. The energy F from (9) satisfies $F \geq 0$, and also we can find two characteristic functions $\chi_1 = \chi_{E_1}$ and $\chi_2 = \chi_{E_2}$ with $E_2 \subset E_1$, E_1, E_2 both with finite perimeter in Ω or finite total variations in Ω, such that $F(\chi_1,\chi_2) < \infty$. These two conditions on F will guarantee that the infimum is finite and that there is a minimizing sequence χ^k_1, χ^k_2 defined by $\inf_{\chi_1,\chi_2} F(\chi_1,\chi_2) = \lim_{k\to\infty} F(\chi^k_1,\chi^k_2)$.

Taking such a minimizing sequence (χ^k_1,χ^k_2) of F, as $k \to \infty$, among characteristic functions of sets of finite perimeter in Ω (i.e. with boundary of finite length), based on the lower semi-continuity of the total variation (Evans and Gariepy 1992) [16], we can extract a subsequence, still denoted by (χ^k_1,χ^k_2), such that each χ^k_i converges to $\chi_i \in BV(\Omega)$ strongly in $L^1(\Omega)$, and such that $\int_\Omega |\nabla\chi_i| \leq \liminf_{k\to\infty}\int_\Omega |\nabla\chi^k_i|$. Moreover, the functions χ_i, $i = 1,2$ have to be equal to 0 or 1 almost everywhere, therefore these are characteristic functions of sets of finite perimeter in Ω, and also $\chi_1 \geq \chi_2$.

We also have that c_i are continuous function of χ_i, therefore $\lim_{k\to\infty} c_i(\chi^k_1,\chi^k_2) = c_i(\chi_1,\chi_2)$. Then, we deduce that

$$F(\chi_1,\chi_2) \leq \liminf_{k\to\infty} F(\chi^k_1,\chi^k_2),$$

therefore existence of minimizers among characteristic functions χ_1, χ_2 of sets of finite perimeter in Ω and with $\chi_1 \geq \chi_2$.

Convergence of the approximation of the length term Following (Samson et al. 1999) [32], (Samson et al. 2000) [33], we can also show that our approximating functional $L_\varepsilon(\phi) = \int_\Omega |\nabla H_\varepsilon(\phi)| dx = \int_\Omega \delta_\varepsilon(\phi)|\nabla\phi| dx$ converges to the length $|C|$ of the zero-level line $C = \{x \in \Omega : \phi(x) = 0\}$, under the assumption that $\phi : \Omega \to I\!R$ is Lipschitz. The same result holds for the case of any l-level curve of ϕ, and not only for the 0-level curve.

Lemma: *According to the previous definitions, let us define*

$$L_\varepsilon(\phi) = \int_\Omega |\nabla H_\varepsilon(\phi)| dx = \int_\Omega \delta_\varepsilon(\phi)|\nabla\phi| dx.$$

Then we have

$$\lim_{\varepsilon\to 0} L_\varepsilon(\phi) = \int_{\{\phi=0\}} ds = |C|,$$

where $C = \{\phi = 0\}$.

Proof: Using the Coarea formula (Evans and Gariepy 1992) [16], we have:

$$L_\varepsilon(\phi) = \int_{I\!R} \Big[\int_{\phi=\rho} \delta_\varepsilon(\phi(x)) ds \Big] d\rho = \int_{I\!R} \Big[\delta_\varepsilon(\rho) \int_{\phi=\rho} ds \Big] d\rho.$$

By setting $h(\rho) = \int_{\phi=\rho} ds$, we obtain

$$L_\varepsilon(\phi) = \int_{I\!R} \delta_\varepsilon(\rho) h(\rho) d\rho = \int_{I\!R} \frac{1}{\pi} \frac{\varepsilon}{\varepsilon^2 + \rho^2} h(\rho) d\rho.$$

By the change of variable $\theta = \frac{\rho}{\varepsilon}$, we obtain

$$\begin{aligned} \lim_{\varepsilon\to 0} L_\varepsilon(\phi) &= \lim_{\varepsilon\to 0} \int_{I\!R} \frac{1}{\pi} \frac{\varepsilon^2}{\varepsilon^2 + \varepsilon^2\theta^2} h(\theta\varepsilon) d\theta \\ &= \lim_{\varepsilon\to 0} \int_{I\!R} \frac{1}{\pi} \frac{1}{1+\theta^2} h(\theta\varepsilon) d\theta \\ = h(0) \int_{I\!R} \frac{1}{\pi} \frac{1}{1+\theta^2} d\theta &= h(0) \frac{1}{\pi} \arctan\theta |_{-\infty}^{+\infty} \\ &= h(0) = \int_{\phi=0} ds = |C|, \end{aligned}$$

which concludes the proof.

In general, this convergence result is valid for any approximations H_ε, δ_ε, under the assumptions that $\lim_{\varepsilon\to 0} H_\varepsilon(x) = H(x)$ in $I\!R \setminus \{0\}$, $\delta_\varepsilon = H'_\varepsilon$, $H_\varepsilon \in C^1(I\!R)$, $\int_{-\infty}^{+\infty} \delta_1(x) dx = 1$.

References

[1] L. Ambrosio, L, *A compactness theorem for a special class of functions of bounded variation*, Boll. Un. Mat. It., 3(B):857-881, 1989.

[2] L. Ambrosio, V.M. Tortorelli, *Approximation of functionals depending on jumps by elliptic functionals via* Γ*-convergence*, Comm. Pure Appl. Math., 43, 999-1036, 1990.

[3] L. Ambrosio, V.M. Tortorelli, *On the Approximation of Free Discontinuity Problems*, Bollettino U.M.I. (7) 6-B, 105-123, 1992.

[4] G. Aubert and P. Kornprobst, *Mathematical Problems in Image Processing. Partial Differential Equations and the Calculus of Variations*. Applied Mathematical Sciences. VOL. 147, Springer, 2001.

[5] R.E. Caflisch, M.F. Gyure, B. Merriman, S. Osher, C. Ratsch, D.D. Vvedensky, and J.J. Zinck, *Island Dynamics and the Level Set Method for Epitaxial Growth*, Applied Mathematics Letters 12, Issue 4, p. 13, 1999.

[6] V. Caselles, F. Catté, T. Coll, F. Dibos, *A geometric model for active contours in image-processing*, Numerische Mathematik, 66 (1): 1-31, 1993.

[7] V. Caselles, R. Kimmel, G. Sapiro, *Geodesic active contours*, IJCV 22 (1): 61-79, 1997.

[8] A. Chambolle, *Image segmentation by variational methods: Mumford and Shah functional and the discrete approximations*, SIAM J. Appl. Math., 55(3):827-863, 1995.

[9] A. Chambolle, *Finite-differences discretizations of the Mumford-Shah functional*. M2AN Math. Model. Numer. Anal., 33(2):261-288, 1999.

[10] T. F. Chan and L. Vese, *An active contour model without edges*, in "Scale-Space Theories in Computer Vision", Lecture Notes in Computer Science Vol. 1682 , pp. 141-151, 1999.

[11] T.F. Chan and L.A. Vese, *Active contours without edges*, IEEE Transactions on Image Processing, Vol. 10(2), pp. 266 -277, 2001.

[12] T.F. Chan and L.A. Vese, *Level Set Algorithm for Minimizing the Mumford-Shah Functional in Image Processing*, IEEE Workshop on Variational and Level Set Methods, pp. 161 -168, 2001.

[13] S. Chen, M. Kang, B. Merriman, R.E. Caflisch, C. Ratsch, R. Fedkiw, M.F. Gyure, and S. Osher, *Level Set Method for Thin Film Epitaxial Growth*, Journ. Comp. Phys. Vol. 167, 475, 2001.

[14] G. Congedo and I. Tamanini, *Density theorems for local minimizers of area type functionals*.

[15] G. Dal Maso, J. Morel, and S. Solimini, *A variational method in image segmentation: existence and approximation results*. Acta Matematica, 168:89-151, 1992.

[16] L.C. Evans and R. Gariepy, *Measure Theory and Fine Properties of Functions*. CRC Press, 1992.

[17] S. Kichenassamy, A. Kumar, P. Olver, A. Tannenbaum, A. Yezzi Jr., *Conformal curvature flows: from phase transitions to active vision*, Arch. Rational Mech. Anal. 134 (1996), no. 3, 275–301.

[18] G. Koepfler, C. Lopez and J.-M. Morel, *A multiscale algorithm for image segmentation by variational method*, SIAM J. Num. Analysis, 31(1), pp. 282-299, 1994.

[19] R. Malladi, J.A. Sethian, and B.C. Vemuri, *Shape modeling with front propagation - a level set approach*, IEEE Tr. PAMI, 17 (2): 158-175, 1995.

[20] J. Lie, M. Lysaker and X.-C. Tai, *A Binary Level Set Model and Some Applications to Mumford-Shah Image Segmentation*, UCLA CAM Report 04-31, May 2004.

[21] B. Merriman, J.K. Bence, and S. Osher, *Motion of Multiple Junctions: A Level Set Approach.* Journal of Computational Physics, 112(2):334-363, 1994.

[22] J. Morel and S, Solimini, *Segmentation of images by variational methods: a constructive approach.* Revista Matematica Universidad Complutense de Madrid, 1:169-182, 1988.

[23] J. Morel and S, Solimini, *Segmentation d'images par méthode variationnelle: une preuve constructive d'existence.* C.R. Acad. Sci. Paris Série I, Math., 308:465-470, 1989.

[24] J. Morel and S, Solimini, *Density estimates for the boundaries of optimal segmentations*, CRASS I-Mathématique, 312 (6): 429-432, 1991.

[25] J. Morel and S, Solimini, *Variational Methods in Image Segmentation.* Birkhäuser, PNLDE 14, 1994.

[26] D. Mumford and J. Shah, *Optimal approximation by piecewise smooth functions and associated variational problems*, Comm. Pure Appl. Math., 42:577-685, 1989.

[27] S.Osher and R. Fedkiw, *Level set methods and dynamic implicit surfaces.*Applied Mathematical Sciences, 153. Springer-Verlag, New York, 2003.

[28] S. Osher and J. Sethian, *Fronts propagating with curvature-dependent speed - Algorithms based on Hamilton-Jacobi formulations*, JCP 79 (1): 12-49, 1988.

[29] N. Paragios and R. Deriche, *Unifying boundary and region-based information for geodesic active tracking*, Proceedings, Computer Vision and Pattern Recognition, 1999, Volume 2, 23-25 June 1999.

[30] N. Paragios and R. Deriche, *Geodesic active regions: A new framework to deal with frame partition problems in computer vision*, Journal of Visual Communication and Image Representation, 13(1-2): 249-268, 2002.

[31] N. Paragios and R. Deriche, *Geodesic active regions and level set methods for supervised texture segmentation*, IJCV 46(3): 223-247, 2002.

[32] C. Samson, L. Blanc-Féraud, G. Aubert, J. Zérubia, *A level set model for image classification*, LNCS Vol. 1682, 306-317, 1999.

[33] C. Samson, L. Blanc-Féraud, G. Aubert, J. Zérubia, *A level set model for image classification*, IJCV 40 (3): 187-197, 2000.

[34] A. Tsai, A. Yezzi, A.S. Willsky, *Curve evolution implementation of the Mumford-Shah functional for image segmentation, denoising, interpolation, and magnification*, IEEE Transactions on Image Processing, 10(8):1169 - 1186, 2001.

[35] L.A. Vese and T.F. Chan, *A Multiphase Level Set Framework for Image Segmentation Using the Mumford and Shah Model*, International Journal of Computer Vision 50(3), 271-293, 2002.

[36] L. Vese, *Multiphase Object Detection and Image Segmentation* in "Geometric Level Set Methods in Imaging, Vision and Graphics", S. Osher and N. Paragios (eds), Springer Verlag, 2003, pp. 175-194.

[37] H.-K. Zhao, T. Chan, B. Merriman, and S. Osher, *Variational level set approach to multiphase motion*, Journal of Computational Physics, 127 (1): 179-195, 1996.